Virus Research 273 (2019) 197756

Contents lists available at ScienceDirect

Virus Research

journal homepage: www.elsevier.com/locate/virusres

HIV-1 Tat protein inhibits the hematopoietic support function of human bone marrow mesenchymal stem cells

Yahong Yuan[a,1], Chunfang Zhou[b,1], Qi Yang[c], Shinan Ma[a], Xiaoli Wang[a], Xingrong Guo[a], Yan Ding[a], Junming Tang[a], Yi Zeng[d], Dongsheng Li[a,*]

[a] Hubei Key Laboratory of Embryonic Stem Cell Research, Taihe Hospital, Hubei University of Medicine, 32 S. Renmin Rd., Shiyan, Hubei, 442000, China
[b] Department of Gastroenterology, Renmin Hospital, Hubei University of Medicine, Shiyan, Hubei, 442000, China
[c] Department of Spinal Surgery, Taihe Hospital, Hubei University of Medicine, Shiyan, Hubei, 442000, China
[d] College of Life Science and Bioengineering, Beijing University of Technology, Beijing, 100124, China

ARTICLE INFO

Keywords:
Tat
HIV-1
Bone marrow mesenchymal stem cells
Hematopoiesis
Hematopoietic stem cells

ABSTRACT

Most HIV-1-infected patients experience hematopoiesis suppression complications. Bone marrow mesenchymal stem cells (BMSCs) are involved in regulation of hematopoietic homeostasis, so we investigated the role of Tat, a protein released by infected cells in bone marrow and impacted differentiation potential of mesenchymal stem cells, in the BMSC hematopoietic support function. BMSCs were treated with HIV-1 Tat protein ($BMSC_{Tat\text{-}p}$), transfected with HIV-1 Tat mRNA ($BMSC_{Tat\text{-}m}$) or treated with solvent (PBS) ($BMSC_{con}$) for 20 days. Then, the hematopoietic support function of $BMSC_{Tat\text{-}p}$, $BMSC_{Tat\text{-}m}$ and $BMSC_{con}$ was analyzed *via* ex vivo expansion of hematopoietic stem cells (HSCs) grown on the BMSCs and *via* in vivo cotransplantation of HSCs and BMSCs. In addition, the hematopoiesis-supporting gene expression patterns of $BMSC_{Tat\text{-}p}$, $BMSC_{Tat\text{-}m}$ and $BMSC_{con}$ were compared. The results showed that $BMSC_{Tat\text{-}p}$ and $BMSC_{Tat\text{-}m}$ displayed reduced expansion, a decline in the number of colony forming units (CFUs) and a decreased proportion of the primitive subpopulation of hematopoietic stem cells under coculture conditions compared with $BMSC_{con}$. The ability of $BMSC_{Tat\text{-}p}$ to support hematopoietic recovery was also impaired, which was further confirmed by the patterns in gene expression analysis. In conclusion, Tat treatment reduced the function of BMSCs in hematopoietic support, likely by downregulating the expression of a series of hematopoietic cytokines.

1. Introduction

Although human immunodeficiency virus type 1 (HIV-1) infection is primarily characterized by the typical deficit in $CD4^+$ T lymphocytes, deficiencies in other hematopoietic lineages are also frequently observed in some HIV-infected patients (Sloand, 2005; Scott, 2010). Cytopenia (anemia, eutropenia, thrombocytopenia) is one of the most common complications of HIV-1 (Opie, 2012). In addition to some secondary complications of HIV-1 infection, such as antiviral medication, infection, inflammation, malignancy and polypharmacy, HIV-1 infection can lead to hematopoietic suppression, indicating that HIV-1 itself is involved in hematopoiesis impairment (Redig and Berliner, 2013). Broadly, hematopoietic stem/progenitor cells (HSPCs) barely can be infected by HIV-1, HIV-1 can exert hematopoietic suppression mainly through indirect mechanisms. Bone marrow (BM) microenvironment injury caused by HIV-1 virus or HIV-1 proteins can indirectly impair hematopoietic homeostasis. It has been shown that HIV-1 replication in the stroma cell monolayers in long-term BM culture (LTBMC) in vitro causes a decrease in hematopoietic cell production (Bahner et al., 1997). In addition, proteins released by an HIV reservoir in the BM can activate inflammatory pathway factors to exert deleterious effects on the BM milieu, which HSCs depend on for survival (Kuller et al., 2008). However, the BM milieu is a heterogeneous cell population that includes fibroblasts, endothelial cells, adipocytes, macrophages, osteoclasts, reticular cells and especially bone marrow mesenchymal stem cells (BMSCs) (Bahner et al., 1997), which play an indispensable role in maintaining the balance of normal hematopoiesis. BMSCs, the important component and regulator of bone marrow microenvironment, give rise to hematopoietic-supporting stromal cells and form hematopoietic niches for hematopoietic stem cells (HSCs) (Morrison and Scadden, 2014.). In addition, BMSCs supply cytokines, adhesion molecules, and extracellular matrix proteins to

* Corresponding author.
E-mail address: 20090098@hbmu.edu.cn (D. Li).
[1] Yahong Yuan and Chunfang Zhou contributed equally to this work.

https://doi.org/10.1016/j.virusres.2019.197756
Received 16 July 2019; Received in revised form 11 September 2019; Accepted 11 September 2019
Available online 12 September 2019
0168-1702/

regulateproliferation and differentiation of HSCs (Anthony and Link, 2014; Ehninger and Trumpp, 2011). Although BMSCs express the CD4 coreceptors CCR5 and CXCR4, these cells do not seem susceptible to HIV infection; integrated proviruses are rarely ever found, and a resulting infection has not yet been discovered (Nazari-Shafti et al., 2011). Whether HIV proteins exert effects on the hematopoietic support function of BMSCs remains unclear.

HIV-1 Tat protein binds the transactivation region (TAR) in the HIV long terminal repeat and affects RNA polymerase activity and function, playing a pivotal role in HIV replication (Wilhelm et al., 2012). Tat protein can be released from infected cells into the extracellular medium (Ju et al., 2012). In addition to its influence on HIV replication, Tat can bind certain cell membrane receptors, such as Flt-1, KDR, integrins, heparan sulfates, and chemokine receptors (Morini et al., 2000; Gibellini et al., 2005; Park et al., 2001), and enter HIV-1-infected or uninfected cells to activate signal transduction pathways and affect the biological characteristics of cells. Tat protein affects the survival, proliferation, and function of several cell lineages, such as T lymphocytes, macrophages, neurons, and endothelial cells (Fanales-Belasio et al., 2009; Guedia et al., 2016; Johnson et al., 2013). Moreover, some reports have demonstrated that mesenchymal stem cells (MSCs) chronically treated with Tat have reduced proliferative activity and undergo early senescence associated with a change in their differentiation potential (Beaupere et al., 2015; Cotter et al., 2008, 2011; Gibellini et al., 2010, 2012). Cytopenias impede anti-viral therapy and play a significant role in the morbidity associated with HIV, such as the opportunistic infections and neoplasms of AIDS. To better understand the pathophysiology of hematopoiesis failure in patients with HIV-1 infection, we studied the effects of Tat on the BMSC hematopoietic support function and analyzed whether Tat may be involved in the hematopoiesis suppression observed in HIV-infected patients. This study provides preliminary evidence for a better understanding of the functional status of BMSCs in HIV patients and the role of Tat in BMSC function.

2. Materials and methods

2.1. BMSC culture and treatment

Bone marrow was isolated from patients undergoing fracture surgery with informed consent. Experimental procedures were approved by the Taihe Hospital Ethical Committees for clinical research (Shiyan, China). Bone marrow cells obtained after Ficoll separation (Invitrogen Corporation, San Diego, CA, USA) were cultured at an initial density of 5×10^4 cells/cm^2 in alpha-minimum essential medium, supplemented with 10% fetal bovine serum (Hyclone, Perbio Science, Erembodegem-Aalst, Belgium), 2 mmol/L glutamine, 2.5 ng/mL bFGF (R&D Systems, Minneapolis, USA) and Penicillin/Streptomycin (Gibco, Invitrogen Corporation). After 2–3 days, nonadherent cells were removed, the adherent cell culture was continued until cells achieved nearly 80–90% confluence. Then, adherent cells were trypsinized, harvested and cultured by seeding with a density of 5×10^3cells/cm^2. Cultures were refreshed with medium every 2 to 3 days and passaged every 5 days. The analysis of the differentiation potential and the identification of immunophenotypes were carried out and presented in our previous study (Yuan et al., 2017). All experiments were performed on BMSCs isolated from at least three different BM donors. BMSCs were treated with 100 ng/mL recombinant HIV-1 Tat protein (Abcam, England) ($BMSC_{Tat\text{-}p}$), transfected with HIV-1 Tat mRNA ($BMSC_{Tat\text{-}m}$) or treated with the solvent (PBS) ($BMSC_{con}$) for 20 days, from passage 2 to 6. The medium was refreshed every 2 to 3 days.

2.2. Animals

NOD/SCID mice (females, 6–8 weeks of age) were purchased from the Model Animal Research Center at Nanjing University (Nanjing, China) and housed in accordance with the National Institutes of Health Guide for the Care and Use of Laboratory Animals. The experimental protocols used in the present study were approved by the Animal Care Committee at Hubei University of Medicine (Shiyan, China).

2.3. In vitro synthesis of Tat mRNA and BMSC transfection

HIV-1 Tat mRNA synthesis was carried out according to protocols described earlier (Wang et al., 2014). The Tat sequence from the HXB2 strain (Opi et al., 2002) was synthesized commercially by Sangon Biotech (Shanghai, China). Template PCR amplicons were subcloned with the use of a pcDNA 3.3-TOPO TA cloning kit (Invitrogen). Plasmid inserts were excised *via* restriction digestion and used to template tail PCRs. RNA was synthesized with the use of a MEGAscript T7 kit (Ambion, San Diego, CA, USA), and a ribonucleoside blend was used comprising ARCA cap analog (New England Biolabs, Ipswich, MA, USA), adenosine triphosphate, guanosine triphosphate (Ambion), 5-methylcytidine triphosphate and pseudouridine triphosphate (TriLink Biotechnologies, San Diego, CA, USA). Reactions were incubated for 5 h at 37°C followed by DNase treatment according to the manufacturer's instruction. The reactions were then treated with Antarctic Phosphatase (New England Biolabs) for 2 h at 37°C to remove residual 5′-triphosphates. The synthesized RNA was purified by means of Ambion MEGAclear spin columns (Ambion) and quantified with a Nanodrop spectrophotometer (Thermo Scientific, Waltham, MA, USA). RNA transfection was carried out with TransIT-mRNA (Mirus, Madison, WI, USA). RNA was diluted in Opti-MEM basal medium (Gibco), and then, Boost reagent and TransIT-mRNA were added sequentially. After a 2-min incubation at room temperature (RT), the RNA-lipid complexes were delivered to culture medium. Four h later, the medium was replaced with normal culture medium. In the 20-day treatment process, transfection was repeated every 3 days.

2.4. Western blot analysis

BMSCs transfected with Tat mRNA were washed with PBS three times and collected with cell lysis buffer. Cell lysates were incubated on ice for 30 min. Proteins in the cell lysates were separated *via* 12% sodium dodecyl sulfate (SDS)-polyacrylamide gel electrophoresis and electrotransferred to nitrocellulose membranes. The blot was put in blocking buffer for 1 h at RT followed by incubation with 1:500 rabbit anti-HIV 1 Tat antibody (Abcam, Cambridge, MA, USA) overnight at 4°C. The blots were rinsed with Tris-buffered saline with Tween-20 three times and incubated with mouse anti-rabbit horseradish peroxide-conjugated secondary antibody (1:1000) for 60 min and detected *via* chemiluminescence with ECL Hyperfilm.

2.5. Immunocytochemistry analysis

BMSCs transfected with Tat mRNA were fixed with 4% paraformaldehyde (Sigma) for 10 min and washed three times with PBS. Cells were permeabilized with 0.1% Trion-X 100 (Sigma) for 20 min and blocked with 2% bovine serum albumin at RT for 60 min. The cells were incubated with rabbit anti-HIV 1 Tat antibody (1:500) for 60 min at 37°C. After being rinsed with PBS 3 times, the cells were incubated with Cy3-conjugated mouse anti-rabbit IgG (1:200, Santa Cruz Biotechnology), followed by 3 rinses with PBS. Cell nuclei were counterstained with 4,6-diamidino-2 -phenylindole and examined under a fluorescence microscope (Leica DMIRE2, Solms, Germany).

2.6. Reverse transcriptase polymerase chain reaction (RT-PCR) analysis

Quantitative reverse transcriptase polymerase chain reaction (RT-PCR) was performed to assess the expression of hematopoiesis-regulating genes, including Thrombopoietin (TPO), Flt-3 ligand (Flt3L), stem cell factor (SCF), IL-6, IL-7 and IL-8. Total RNA was extracted from

2×10^5 $BMSC_{Tat\text{-}p}$, $BMSC_{Tat\text{-}m}$ and $BMSC_{Con}$. cDNA was synthesized using a reverse transcription kit (Takara, China), and PCR amplification was performed using SyBR GREEN (Takara, China). The PCR proceeded as follows: 95 °C for 30 s, then 40 cycles of 95 °C for 30 s, 60 °C for 30 s and 72 °C for 30 s. The fold changes in gene expressions were normalized to β-actin.

2.7. Measurement of hematopoietic cytokine levels in BMSC supernatant via enzyme-linked immunosorbent assay (ELISA)

BMSCs incubated with Tat protein, Tat mRNA or control medium for 20 days were seeded in 24-well culture plates at 50,000 cells per well. Supernatants were collected after 72 h and analyzed using commercially available human IL-6, Flt3L, IL-7 and SCF enzyme-linked immunosorbent assay (ELISA) kits (R&D). The monoclonal antibody specific for IL-6, Flt3L, L-7 or SCF had been precoated onto the microplate. Standards and samples were pipetted into the wells, and the hematopoietic cytokines present bound to the specific monoclonal antibody. After the unbound substances were washed away, an enzyme-linked polyclonal antibody specific for the hematopoietic cytokines was added to the wells. Following a wash to remove any unbound antibody-enzyme reagent, the substrate solution was added, and color developed. The color development was stopped, and the optical density of each well was measured using an ELISA reader. All measurements were performed in duplicate.

2.8. Ex vivo expansion of HSCs on a BMSC layer

$CD34^+$ HSCs were isolated from up to 100 mL of umbilical cord blood using Ficoll–Paque (Invitrogen Corporation, San Diego, CA, USA) density gradient centrifugation. $CD34^+$ cells were then enriched from the buffy coat by immunomagnetic positive selection using a MidiMACS™ system (Miltenyi Biotec, Auburn, CA) according to the manufacturer's instructions. Briefly, the mononuclear cells were labeled with CD34 microbeads and added to a MACS LD column attached to a MidiMACS™ magnetic separator. The LD column was then removed from the MidiMACS™ separator, and the bound $CD34^+$ cells were eluted with a plunger. For the coculture, 3×10^4 $BMSC_{Tat\text{-}p}$, $BMSC_{Tat\text{-}m}$ and $BMSC_{Con}$ treated with mitomycin were plated separately in 24-well plates (Corning Costar, NY) that had been precoated for 24 h with 30% gelatin (2% solution, Sigma–Aldrich, Irvine, Ayrshire, UK). A total of 2×10^3 $CD34^+$ cells were seeded on the BMSCs in 1 mL of serum-supplemented IMDM. Control cultures consisted of hematopoietic cells alone. After five days of coculture, 1 mL of fresh complete medium was added, and the coculture continued for another 5 days. On day 10 of coculture, hematopoietic cells expanded on BMSCs were collected. Adherent hematopoietic cells on the stromal layer were removed by washing five times with PBS and mixed with dissociated hematopoietic cells. Then, the viable cell count, subpopulations of the expanded hematopoietic stem cells and colony formation were analyzed.

Trypan blue viable cell counts. Aliquots of the cultured $CD34^+$ HSCs from the BMSC and control plates were collected and stained with 0.4% Trypan Blue for 1 min at room temperature. The number of live HSCs (unstained) was determined using a hemocytometer.

Colony forming unit (CFU) assay. The cultured hematopoietic cells (1000 cells) from the BMSC and control plates were seeded in 24-well plates containing 0.5 mL of semisolid methylcellulose in Methocult H4435 medium. This medium is a commercial medium from Stem Cell Technologies, Inc. that contains IMDM, BSA, 2-mercaptoethanol, rhSCF, rhG-CSF, rhGM-CSF, rhIL3, rhIL6, rhEPO, and supplements. After 14 days of incubation at 37 °C in 5% CO_2, colonies were scored using standard scoring criteria (Vasko et al., 2016).

Flow cytometric analysis of cell subpopulations. In this experiment, A total of 2×10^3 $CD34^+$ cells were seeded on BMSCs in 1 mL of serum-supplemented IMDM. On day 10 of coculture, aliquots of cells were stained for hematopoietic surface markers. In brief CD34-phycoerythrin (PE), CD33-fluorescein isothiocyanate (FITC), CD38-FITC and CD45-FITC (all from BD, Pharmingen, San Diego, CA) monoclonal antibodies were incubated with cells in PBS/0.1% BSA at room temperature for 30 min. Cells labeled with corresponding isotype-matched IgG were used as controls. Labeled cells were washed twice, suspended in 2% paraformaldehyde and analyzed on a flow cytometer. The expanded hematopoietic stem cell subpopulations were initially gated according to their morphology (forward *vs* side scatter FSC/SSC), and dead cells were excluded from the analysis. Then, the $CD34^+CD38^-$ and $CD34^+CD33^-$ expanded cells were analyzed by flow cytometry after gating on $CD45^+$ cells. At least 40,000 events were acquired for each analysis.

2.9. Cotransplantation of BMSCs and HSCs

After receiving a 2.5 Gy dose of ^{60}Co total radiation, the animals were provided with food supplemented with antibiotics and sterile, acidized drinking water containing amphotericin B (80 mg/l) and ciprofloxacin (80 mg/l). Within 12 h of irradiation, 6 mice in each experimental group were transplanted or cotransplanted with the following number of cells *via* the tail vein: (1) $BMSC_{con}$ + HSC group, 8×10^5 $BMSC_{con}$ + 1×10^5 $CD34^+$ cells; (2) $BMSC_{Tat\text{-}p}$ + HSC group, 8×10^5 $BMSC_{Tat\text{-}p}$ + 1×10^5 $CD34^+$ cells; (3) HSC group, 1×10^5 $CD34^+$ cells; (4) IR group, irradiated mice injected with 0.2 mL physiological saline per mouse. The HSCs for transplantation were freshly isolated from umbilical cord blood.

At 2 and 4 weeks after transplantation, tail vein blood was collected, and the leukocyte counts were examined. At 4 weeks after transplantation, mice from each group were anesthetized with isoflurane and sacrificed by cervical dislocation. Peripheral blood samples from mice were stained with anti-human CD45 antibody and analyzed *via* FCM. BM cells from the mouse tibia were harvested. Engraftment of human cells was evaluated by FCM immunophenotyping with FITC-labeled anti-human CD45 antibody, PE-labeled anti-human CD33 antibody and PE-labeled anti-human CD19 antibody (eBioscience, USA). The BM cells from mouse tibias and femurs were harvested for cytology analysis with Wright staining.

2.10. Statistical analysis

All results that are expressed as the mean ± SEM were obtained from more than three samples per experiment, and significant differences between different groups were calculated using a two-tailed Student's *t*-test (SPSS 13). A value of $P < 0.05$ was considered statistically significant.

3. Results

3.1. Efficient transfection of BMSCs with tat mRNA

To confirm that the synthesized Tat mRNA can enter BMSCs and then be translated into Tat protein, BMSCs were transfected with Tat mRNA followed by Tat protein detection through immunostaining. Tat protein expression was detected *via* immunofluorescence in the BMSCs 8 h after transfection. Fig.1a shows that the Tat mRNA entered the BMSCs and was translated into protein in the endochylema. Tat protein expression was also confirmed by Western blotting (Fig.1b).

3.2. Growth states of HSCs when cultured with BMSCs

Live cell counts. After being cultured under different conditions for 10 days, hematopoietic stem cells were observed under a microscope (Fig. 2a). Suspension cells in $BMSC_{Con}$ + HSC culture environments were dense, circular and exhibited good refraction, but cells in the $BMSC_{Tat\text{-}p}$ + HSC and $BMSC_{Tat\text{-}m}$ + HSC groups were slightly sparse, and a small amount of debris was scattered among them. The cells cultured without

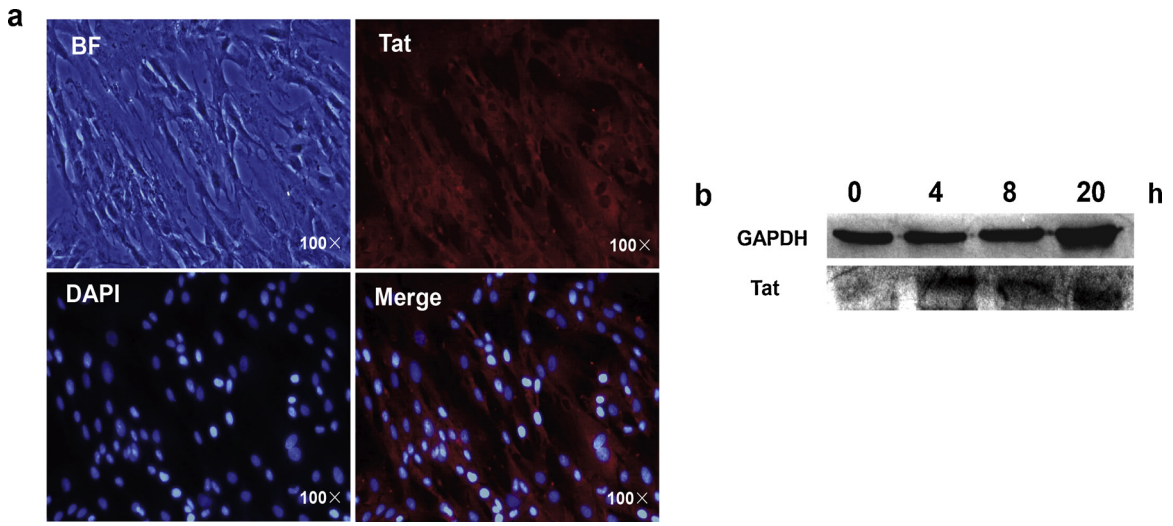

Fig. 1. Efficiency of BMSC transfection with Tat mRNA. BMSCs were treated with Tat mRNA for 8 h, and the expression of Tat was determined by immunofluorescence analysis (× 100) (a). Immunofluorescence images show the intracellular localization of Tat in red and the DAPI-stained nuclei in blue. Western blot detection of Tat protein at 0, 4, 8 and 20 h after transfection of BMSCs with Tat mRNA (b). BMSC extracts were collected with cell lysis buffer, separated *via* SDS–PAGE and transferred onto a nitrocellulose membrane. The membrane was probed with primary antibody for Tat and horseradish peroxidase-conjugated secondary antibody. Then, protein expression was detected using an enhanced chemiluminescence system. DAPI, 4′, 6-diamidino-2- phenylindole; BF, bright field.

BMSCs were almost completely fragmented, apart from a few round hemopoietic cells seen in the central part of the hole. Then, the suspended cells were collected, and Trypan blue staining was used to determine the number of viable and expanded hematopoietic cells. The overall number of live hematopoietic cells in the $BMSC_{Tat\text{-}p}$ + HSC ($35.12 \pm 2.19 \times 10^3$), $BMSC_{Tat\text{-}m}$ + HSC ($22.32 \pm 2.57 \times 10^3$) and HSC alone ($1.23 \pm 0.11 \times 10^3$) culture environments was significantly lower than that in the $BMSC_{con}$ + HSC ($106.55 \pm 17.12 \times 10^3$) culture environment (Fig. 2b).

CFU assay. After 14 days of incubation in Methocult H4435

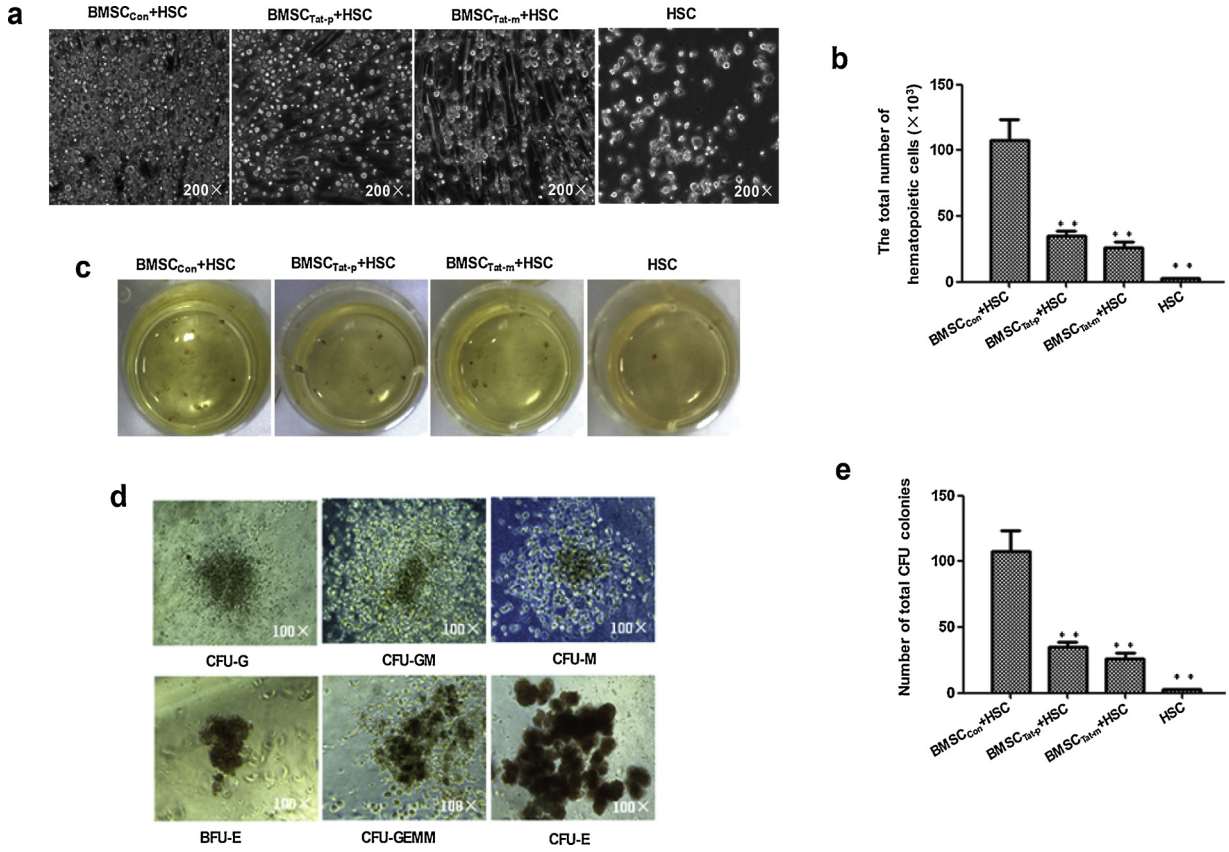

Fig. 2. Expansion of HSCs during coculture with BMSCs after 10 days. The phase contrast image shows different densities of hematopoietic cells on the BMSC feeder layer (a). Nonadherent cells were collected from HSC/BMSC cocultures, and the cell number was determined using trypan blue staining (b). HSCs from different culture environments formed clones in semisolid methylcellulose medium (c). Six different types of colony morphologies were observed (d). The number of total CFU colonies formed under different conditions (e). The mean values of three experiments are shown; *P < 0.05 and **P < 0.01 *vs* BMSC con.

medium, colonies for normal hematopoiesis were observed (Fig. 2c). Colony morphologies were classified according to the manufacturer's manual (Stem Cell Technologies, Inc., Instruction Manual) as colony forming unit-erythroid (CFU-E), colony forming unit-granulocyte (CFU-G), colony forming unit granulocyte/macrophage (CFU-GM), burst forming unit erythroid (BFU-E), colony forming unit-macrophage (CFU-M), and colony forming unit-granulocyte/erythrocyte/macrophage/megakaryocyte (CFU-GEMM) (Fig. 2d). The total colony numbers in the experimental groups were compared. Although the total colony numbers in the $BMSC_{Tat\text{-}p}$ + HSC (28.51 ± 5.13) and $BMSC_{Tat\text{-}m}$ + HSC (22.41 ± 4.17) groups were greater than that in the HSC alone group (7.14 ± 2.43), the numbers were significantly lower than that in the $BMSC_{con}$ + HSC group (86.21 ± 11.54) (Fig. 2e).

Immunophenotype assay of the expanded HSCs. To evaluate the support function of BMSCs toward more primary HSCs ($CD34^+CD33^-$ and $CD34^+CD38^-$ subpopulations), the suspension cells in three groups were assayed *via* flow cytometry. HSCs cultured without BMSCs could not be detected by flow cytometry because most of the cells were dead and broken. The percentage of $CD34^+$CD33- cells cultured under $BMSC_{Con}$ + HSC conditions (25.83 ± 4.73) was higher than that of cells cultured under $BMSC_{Tat\text{-}p}$ + HSC (0.57 ± 0.05) and $BMSC_{Tat\text{-}m}$ + HSC (1.37 ± 0.06) conditions (Fig. 3a and b). Additionally, the percentage of $CD34^+CD38^-$ cells cultured under $BMSC_{Con}$ + HSC conditions (21.83 ± 4.95) was higher than that of cells cultured under $BMSC_{Tat\text{-}p}$ + HSC (0.97 ± 0.06) and $BMSC_{Tat\text{-}m}$ + HSC (1.57 ± 0.07) conditions (Fig. 3a and c). Comparison of the percentage of $CD34^+$ cells in all groups demonstrated a tendency similar to that observed with $CD34^+CD33^-$ cells (Fig. 3a and d).

3.3. Hematopoietic reconstitution after cotransplantation of $CD34^+$ HSCs and BMSCs

Monitoring of peripheral blood. We examined hematopoietic reconstruction in sublethal-dose-irradiated NOD/SCID mice transplanted with human $CD34^+$ HSCs and BMSCs. On the 14th and 28th day after transplantation, white blood cells were counted in the peripheral blood collected from each group. On the 14th day, compared with normal mice (2.46 ± 0.45 × 10^9/ L), the number of white blood cells in the IR group decreased significantly (0.15 ± 0.18 × 10^9/ L), indicating that irradiation seriously damaged the hematopoietic system of NOD/SCID

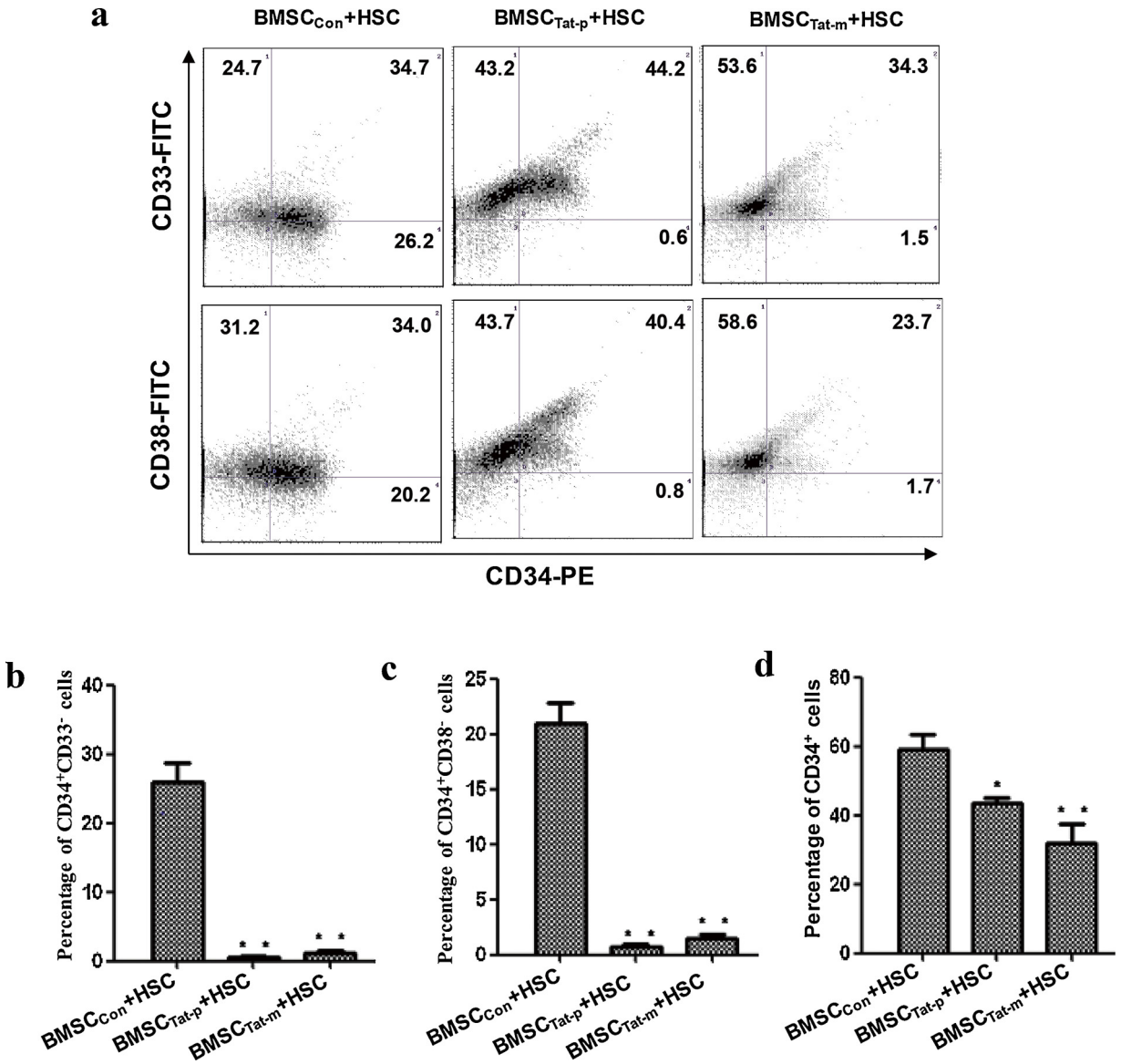

Fig. 3. Flow cytometric analysis of $CD34^+$, $CD34^+CD33^-$, and $CD34^+CD38^-$ cells performed on the $CD45^+$ population under the indicated culture conditions. Representative plots of the flow cytometric analysis are shown (a). Histogram comparing the percentages of $CD34^+CD33^-$ (b), $CD34^+CD38^-$ (c), and $CD34^+$(d) subpopulations. The mean values of three experiments are shown; *P < 0.05 and **P < 0.01 vs BMSCcon.

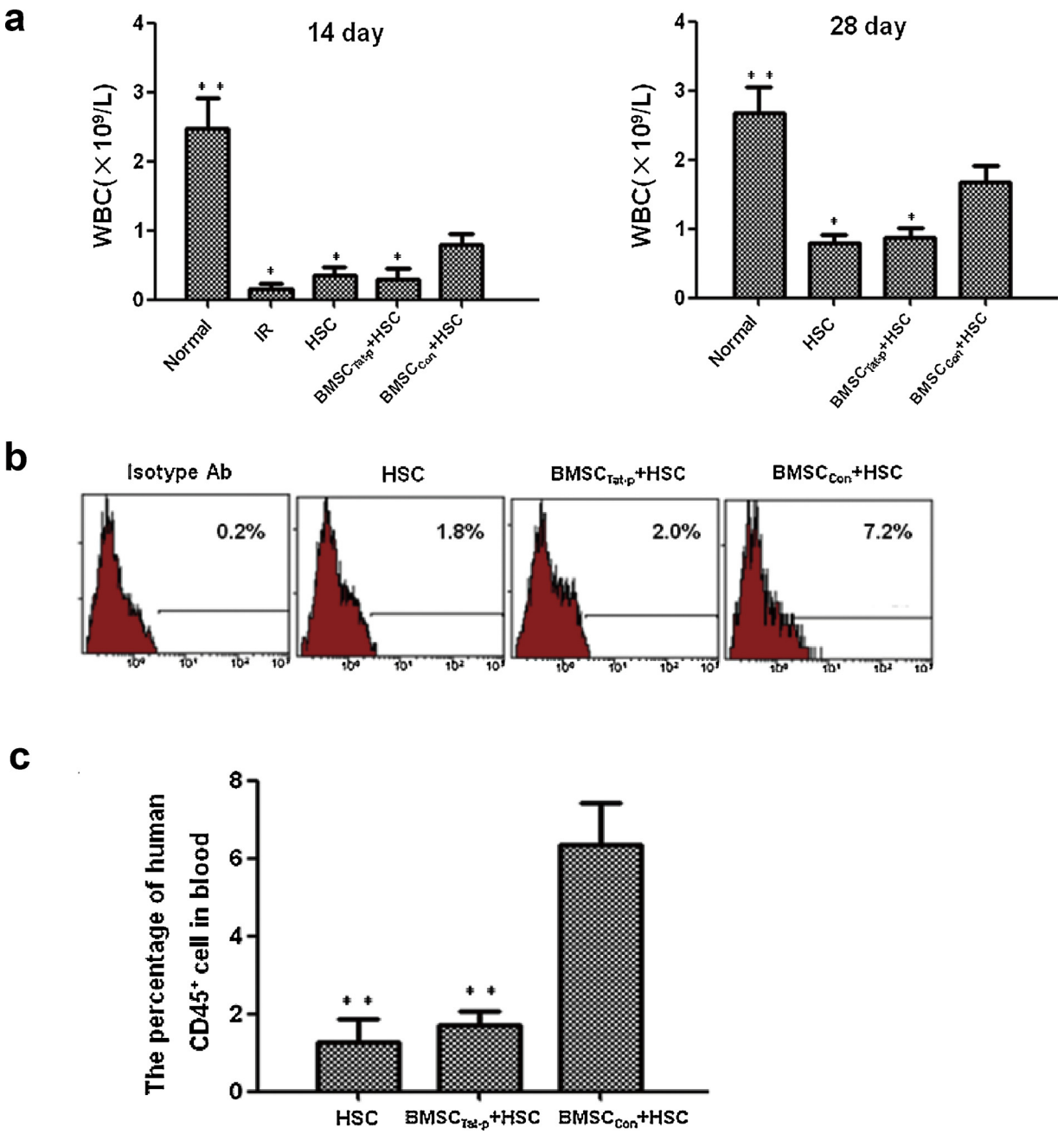

Fig. 4. Recovery of peripheral hematogenesis in irradiated mice following cell transplantation. At 2 and 4 weeks post transplantation with the indicated cell types, leucocyte counts were performed in mice from each group (blood was harvested from the tail vein) (a). Only one mouse was still alive in the IR group at 4 weeks post irradiation, and thus, no statistical data are shown. At 4 weeks post transplantation, PBMCs from the indicated groups were evaluated for the presence of human $CD45^+$ cells *via* FCM. Representative results of three independent experiments are shown (b). The statistical analyses are displayed (c). PBMCs, peripheral blood mononuclear cells; FCM, flow cytometry; IR group, irradiated mice injected with saline. The mean values of three experiments are shown; *P < 0.05 and **P < 0.01 *vs* BMSC con.

mice. Compared with the IR group, the number of white blood cells was recovered after transplantation, and the number in the $BMSC_{Con}$ +HSC group (0.76 ± 0.16 × 10^9/L) was significantly higher than that in the $BMSC_{Tat\text{-}p}$ +HSC group (0.30 ± 0.14 × 10^9/L) and HSC (0.34 ± 0.12 × 10^9/L) (Fig. 4a). By the 28th day, only one mouse was still alive in the IR group, and thus, statistical analysis was not performed. The number of white blood cells in the surviving mice after transplantation increased further but was still lower than that in the normal mice (2.67 ± 0.37 × 10^9/L). The white blood cell number in the $BMSC_{Con}$+ HSC group (1.67 ± 0.23 × 10^9/L) was obviously higher than that in the HSC (0.79 ± 0.13 × 10^9/L) and $BMSC_{Tat\text{-}p}$ +HSC (0.87 ± 0.14 × 10^9/L) groups (Fig. 4a). Then, PBMCs in peripheral blood were detected with flow cytometry on the 28th day after transplantation. Flow cytometry showed that the percentage of human $CD45^+$ cells in each group was lower than 10% (Fig. 4b). Statistical analysis of at least 3 mice in each group showed that although the implantation rate of human hematopoietic cells in the peripheral blood of mice was relatively low, there were still significant differences among the different transplantation groups. The implantation rate in the $BMSC_{Con}$ +HSC group (6.37 ± 1.04%) was obviously higher than that in the HSC (1.27 ± 0.61%) and $BMSC_{Tat\text{-}p}$ +HSC (1.7 ± 0.36%) groups (Fig. 4c).

Bone marrow analysis. Bone marrow cells were collected from all groups, and the percentages of human hematopoietic cells ($CD45^+$),

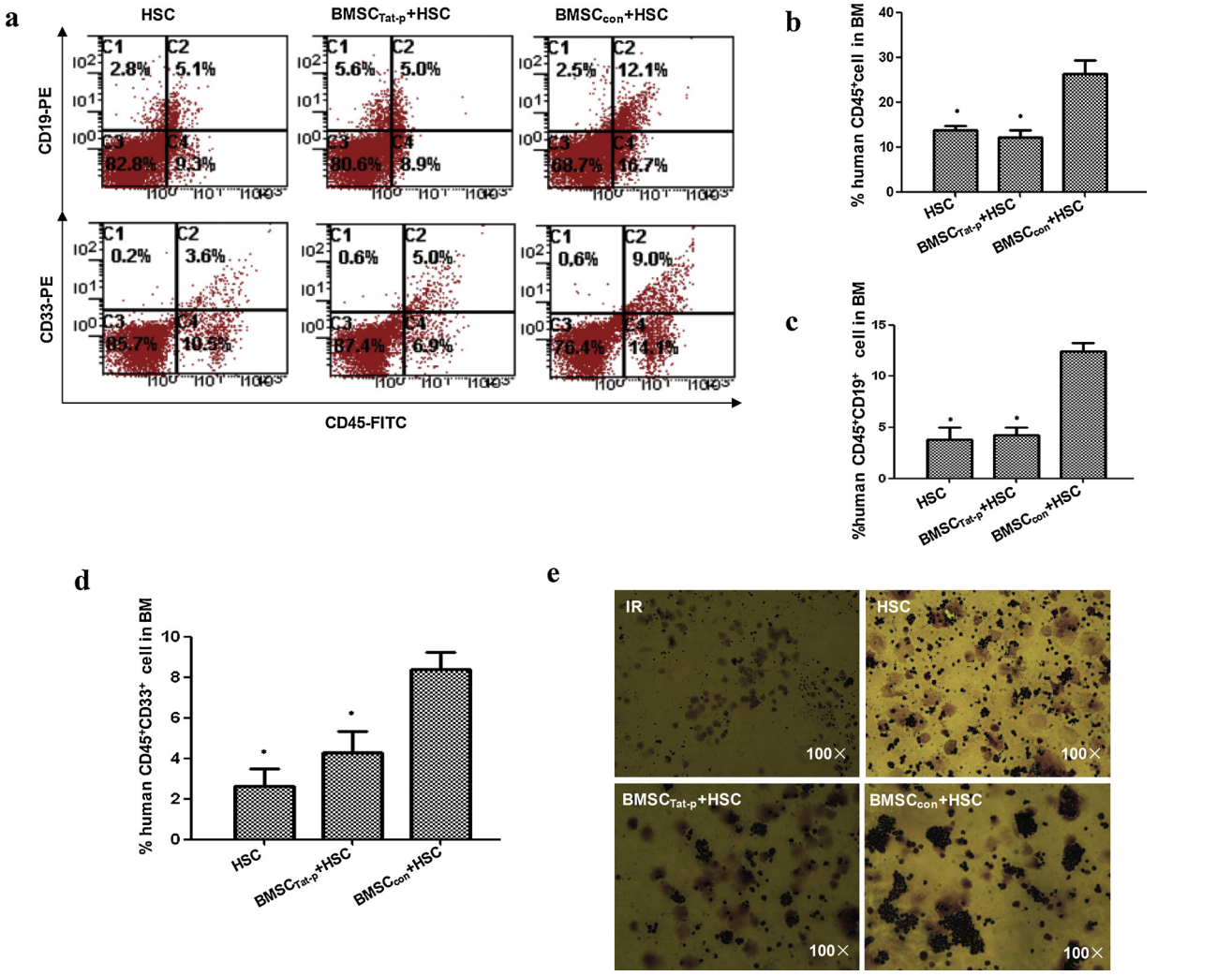

Fig. 5. Recovery of bone marrow hematogenesis in irradiated mice following transplantation. At 4 weeks post transplantation, BM cells from the indicated groups were evaluated for the presence of human $CD45^+$, $CD19^+$ and $CD33^+$ cells *via* FCM. Representative plots of the flow cytometric analysis are shown (a). Histogram comparing the percentages of $CD45^+$ (b), $CD45^+CD19^+$ (c), and $CD45^+CD33^+$ (d) subpopulations. Only one mouse was still alive in the IR group at 4 weeks post irradiation, and thus, no statistical data are shown. Bone marrow cytology results from all groups are displayed (e). BM, bone marrow; FCM, flow cytometry; IR group, irradiated mice injected with saline. The data are displayed as the mean ± standard deviation; *P < 0.05 and **P < 0.01 *vs* BMSC con.

myeloid cells ($CD45^+CD33^+$) and B cells ($CD45^+CD19^+$) were assayed *via* flow cytometry (Fig. 5a). $CD45^+$ cell, $CD45^+CD33^+$ cell and $CD45^+CD19^+$ cell recovery was significantly increased in the $BMSC_{con}$ + HSC group compared with the $BMSC_{Tat\text{-}p}$ + HSC group ($CD45^+$ cells 26.33 ± 2.92 *VS*. 12.06 ± 1.76; myeloid cells 8.37 ± 1.93 *VS*. 4.35 ± 0.75; B-cells 12.43 ± 1.56 *vs*. 4.27 ± 0.85; Fig. 5b–d). To understand bone marrow reconstitution more intuitively, bone marrow smears from each group were observed under a microscope. The bone marrow smears from the IR group showed more cell fragments, the number of hematopoietic cells was very small, and bone marrow hyperplasia was extremely weakened. In the $BMSC_{Con}$ + HSC group, more nucleated cells and fewer cell fragments were observed, many different types of hematopoietic cells could be seen, and myeloproliferation was more active. The number of nucleated cells in the HSC and $BMSC_{Tat\text{-}p}$ + HSC groups was lower than that in the $BMSC_{Con}$ + HSC group, with a small number of cell fragments and low myeloproliferative activity (Fig. 5e).

3.4. Expression of hematopoietic cytokines by BMSCs

RT-PCR was applied to quantify the expression level of TPO, Flt3L, SCF, IL-6, IL-7 and IL-8. The results are expressed after normalization to the expression value of the actin reference gene. Both treated BMSCs and control BMSCs expressed the key genes studied (Fig. 6a). Except IL-6, the expression levels of all these genes in $BMSC_{Tat\text{-}p}$ and $BMSC_{Tat\text{–}m}$ were significantly decreased compared with those in $BMSC_{con}$ (Fig. 6b). The levels of Flt3L, SCF, and IL-6 were decreased in $BMSC_{Tat\text{-}p}$ and $BMSC_{Tat\text{–}m}$ compared with $BMSC_{con}$. There were no significant differences in IL-7 concentration between $BMSC_{Tat\text{-}p}$, $BMSC_{Tat\text{–}m}$ and $BMSC_{con.}$ (Fig. 6c).

4. Discussion

HIV-1 Tat protein has active biological effects on several cell lineages and promotes the pathological process of acquired immune deficiency syndrome (AIDS) (Fanales-Belasio et al., 2009; Guedia et al., 2016; Johnson et al., 2013). Some recent studies have shown that HIV-1 Tat can impact certain basic biological characteristics of MSCs, such as self-renewal capacity and differentiation potential (Beaupere et al., 2015; Cotter et al., 2008; Gibellini et al., 2010, 2012). In this report, we analyzed the effects of Tat on the hematopoietic support function of BMSCs. The results of our study demonstrated that (i) Tat reduced the capacity of BMSCs to support expansion of hematopoietic stem cells in vitro; (ii) Tat-treated BMSCs lost their ability to assist hematopoietic

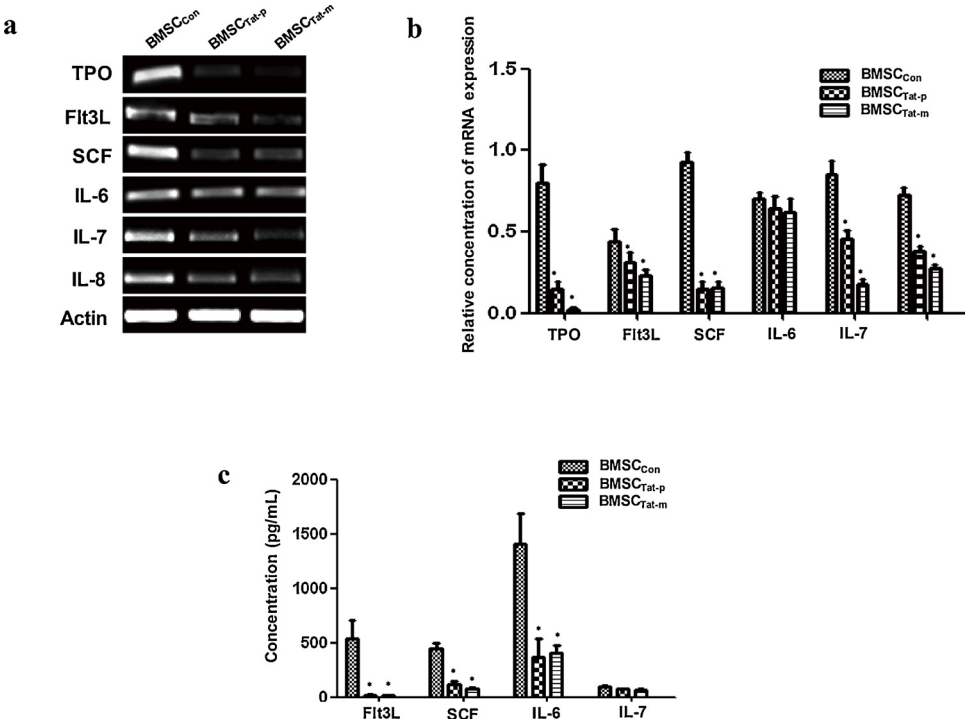

Fig. 6. Hematopoietic cytokines expressed by BMSCs were assayed *via* RT-PCR and ELISA. Hematopoietic cytokine mRNA levels were measured using RT-PCR (a, b). Soluble hematopoietic cytokines secreted in the supernatant of BMSCs were determined *via* ELISA (c). n = 3, and the data are displayed as the mean ± standard deviation; *P < 0.05 and **P < 0.01 *vs* BMSC con.

recovery after cotransplantation of $CD34^+$ HSCs and BMSCs in vivo; and (iii) Tat decreased the expression level of a series of key hematopoietic factors produced by BMSCs. Based on these results, we propose that Tat protein can inhibit the hematopoietic support function of BMSCs, providing new insight into the hematopoietic suppression observed in HIV-infected patients.

Numerous reports have demonstrated the capacity of BMSCs to support the survival, proliferation, and differentiation of HSCs in vitro (Isern et al., 2013; Futrega et al., 2017). In this study, BMSCs were transfected with Tat mRNA or cultured with medium containing Tat protein, and then, the treated BMSCs were used as a feeder layer to support HSC expansion in vitro. We observed that Tat treatment caused reduced expansion, a decline in the number of CFUs and a decreased proportion of the primitive subpopulation of hematopoietic stem cells under coculture conditions. Considering that MSCs express a wide array of hematopoietic cytokines to maintain HSCs in quiescence or promote their self-renewal or proliferation, we compared the gene expression patterns of these cytokines in Tat-treated BMSCs with those in control BMSCs. The cytokine profile, which included TPO, SCF, Flt3L, IL-6, IL-7 and IL-8, of BMSCs assayed in this study confirmed the crucial role of BMSCs in HSPC maintenance (Askmyr et al., 2009; Hermouet et al., 2000; Hofmeister et al., 2007; Ivanovic and Boiron, 2009; Weimar et al., 1998). In the present study, the gene expression level and concentration of these cytokines in the supernatant were dramatically decreased in Tat-treated BMSCs compared with control BMSCs. In addition, several studies have shown that BMSCs possess the ability to promote engraftment and to accelerate hematological recovery after HSC transplantation (Chou et al., 2013; Masuda and Izpisua Belmonte, 2013; Wu et al., 2013). In this study, we cotransplanted Tat-treated BMSCs with HSCs and investigated the degree of human HSC engraftment in irradiated mice. Tat-treated BMSCs led to decreased white blood cell and human $CD45^+$ cell counts in peripheral blood from mice compared with control BMSCs. In addition, we observed that Tat-treated BMSC and HSC cotransplantation led to inferior engraftment of $CD45^+$, $CD33^+$ and $CD19^+$ lineage cells in the bone marrow after 4 weeks compared with the control BMSCs. All of these findings may suggest a decline in the hematopoietic support function of BMSCs caused by Tat treatment, which ultimately could lead to hematopoiesis insufficiency.

MSCs are pluripotent cells capable of differentiating into several mesenchymal cell types, including osteoblasts (OBs) and adipocytes (ACs) (Larrick and Mendelsohn, 2017). The transcription factors peroxisome proliferator-activated receptors gamma (PPARγ) and runt-related transcription factor-2 (RUNX-2) are known to be pro-osteogenic and pro-adipogenic, respectively. Activity of the RUNX-2 transcription factor drives differentiation of OBs from MSCs, while the activity of PPARγ in MSCs induces differentiation into adipocytes (Gimble et al., 2006; Shi et al., 2007). In addition, some studies have shown that (pre) osteoblast differentiation of MSCs stimulates proliferation of hematopoietic precursors, while (pre)osteoblasts progressively disappear in favor of adipocytic cells, which leads to proliferation downregulation. In this process, changes in Runx2 and PPARγ expression correspond to hematopoietic precursor cell numbers (Chitteti et al., 2010; Adler et al., 2014; Poncin et al., 2012; Zhu et al., 2013).

In fact, it has been confirmed that Tat enhances MSC adipogenic differentiation through upregulation of PPARγ and decreases the MSC potential for osteoblastic differentiation, associated with a decrease in RUNX-2 (Gibellini et al., 2012; Geyh et al., 2013). Therefore, Tat impacts the differentiation potential of MSCs by regulating the activities of PPARγ and RUNX-2, which affects the hematopoietic support function of BMSCs.

In this study, we observed that Tat treatment reduced hematopoietic cytokine expression in BMSCs. A recent study has shown that Tat not only alters BMSC differentiation but also promotes early senescence in human BMSCs (Beaupere et al., 2015). Several studies have reported that a reduction of some hematopoietic cytokines produced by MSCs could be induced by senescence. Geyh S showed that MSCs from MDS patients exhibit aging characteristics and altered expression of key molecules, leading to deficient hematopoiesis in MDS (Geyh et al., 2013) Research reported by Huang K showed that the levels of SCF, Flt3L, IL-6 and SDF-1 in BMSCs from 0- to 20-year-old donors were higher than those in BMSCs from 40-year-old or older donors (Huang et al., 2005). Additionally, a report by Tsuboi indicated that a decrease in IL-7 in stromal cells of senescence-accelerated mice led to homeostasis suppression (Tsuboi et al., 2004). Therefore, Tat may affect the production of hematopoietic factors by inducing BMSC aging.

Overall, both the presence of Tat protein in the external environment of BMSCs and transfer of Tat-mRNA into BMSCs inhibited the hematopoietic support function of BMSCs. These results indicate that BMSCs in the bone marrow of HIV patients might fail to perform normal hematopoietic support functions, and Tat protein might be one of the major factors involved in the hematopoiesis abnormalities of HIV patients. This would suggest that the status of bone marrow MSCs should be taken into consideration when HIV patients are treated.

Declaration of Competing Interest

The authors declare that they have no conflicts of interest.

Acknowledgments

This study was supported by the Knowledge Innovation Program of Science and Technology Department of Hubei Province (Hubei Provincial Natural Science Foundation , 2019CFB289) , Science and Technology Department Foundation of Hubei Province(2018ACA162) and the Major Science and Technology Project of Hubei Province (2016ACA157)

References

Adler, B.J., Kaushansky, K., Rubin, C.T., 2014. Obesity-driven disruption of haematopoiesis and the bone marrow niche. Nat. Rev. Endocrinol. 10 (12), 737–748.
Anthony, B.A., Link, D.C., 2014. Regulation of hematopoietic stem cells by bone marrow stromal cells. Trends Immunol. 35 (1), 32–37.
Askmyr, M., Sims, N.A., Martin, T.J., Purton, L.E., 2009. What is the true nature of the osteoblastic hematopoietic stem cell niche? Trends Endocrinol. Metab. 20 (6), 303–309.
Bahner, I., Kearns, K., Coutinho, S., Leonard, E.H., Kohn, D.B., 1997. Infection of human marrow stroma by human immunodeficiency virus-1 (HIV-1) is both required and sufficient for HIV-1–induced hematopoietic suppression in vitro: demonstration by gene modification of primary human stroma. Blood 90 (5), 1787–1798.
Beaupere, C., Garcia, M., Larghero, J., Fève, B., Capeau, J., Lagathu, C., 2015. The HIV proteins Tat and Nef promote human bone marrow mesenchymal stem cell senescence and alter osteoblastic differentiation. Aging Cell 14 (4), 534–546.
Chitteti, B.R., Cheng, Y.H., Poteat, B., Rodriguez-Rodriguez, S., Goebel, W.S., Carlesso, N., Kacena, M.A., Srour, E.F., 2010. Impact of interactions of cellular components of the bone marrow microenvironment on hematopoietic stem and progenitor cell function. Blood 115 (16), 3239–3248.
Chou, S.H., Lin, S.Z., Day, C.H., Kuo, W.W., Shen, C.Y., Hsieh, D.J., Lin, J.Y., Tsai, F.J., Tsai, C.H., Huang, C.Y., 2013. Mesenchymal stem cell insights: prospects in hematological transplantation. Cell Transplant. 22 (4), 711–721.
Cotter, E.J., Chew, N., Powderly, W.G., Doran, P.P., 2011. HIV 1 alters mesenchymal stem cell differentiation potential and cell phenotype ex vivo. AIDS Res. Hum. Retroviruses 27 (2), 187–199.
Cotter, E.J., Ip, H.S., Powderly, W.G., Doran, P.P., 2008. Mechanism of HIV protein induced modulation of mesenchymal stem cell osteogenic differentiation. BMC Musculoskelet. Disord. 9, 33.
Ehninger, A., Trumpp, A., 2011. The bone marrow stem cell niche grows up:mesenchymal stem cells and macrophages move in. J. Exp. Med. 208 (3), 421–428.
Fanales-Belasio, E., Moretti, S., Fiorelli, V., Tripiciano, A., Pavone Cossut, M.R., Scoglio, A., Collacchi, B., Nappi, F., Macchia, I., Bellino, S., Francavilla, V., Caputo, A., Barillari, G., Magnani, M., Laguardia, M.E., Cafaro, A., Titti, F., Monini, P., Ensoli, F., Ensoli, B., 2009. HIV-1 Tat addresses dendritic cells to induce a predominant Th1-type adaptive immune response that appears prevalent in the asymptomatic stage of infection. J. Immunol. 182 (5), 2888–2897.
Futrega, K., Atkinson, K., Lott, W.B., Doran, M.R., 2017. Spheroid coculture of hematopoietic stem/progenitor cells and monolayer expanded mesenchymal stem/stromal cells in polydimethylsiloxane microwells modestly improves in vitro hematopoietic stem/progenitor cell expansion. Tissue Eng. Part C Methods 23 (4), 200–218.
Geyh, S., Oz, S., Cadeddu, R.P., Fröbel, J., Brückner, B., Kündgen, A., Fenk, R., Bruns, I., Zilkens, C., Hermsen, D., Gattermann, N., Kobbe, G., Germing, U., Lyko, F., Haas, R., Schroeder, T., 2013. Insufficient stromal support in MDS results from molecular and functional deficits of mesenchymal stromal cells. Leukemia 27 (9), 1841–1851.
Gibellini, D., Vitone, F., Schiavone, P., Re, M.C., 2005. HIV-1 Tat protein and cell proliferation and survival: a brief review. New Microbiol. 28 (2), 95–109.
Gibellini, D., De Crignis, E., Ponti, C., Borderi, M., Clò, A., Miserocchi, A., Viale, P., Re, M.C., 2010. HIV-1 Tat protein enhances RANKL/M-CSF-mediated osteoclast differentiation. Biochem. Biophys. Res. Commun. 401 (3), 429–434.
Gibellini, D., Miserocchi, A., Tazzari, P.L., Ricci, F., Clò, A., Morini, S., Ponti, C., Pasquinelli, G., Bon, I., Pagliaro, P., Borderi, M., Re, M.C., 2012. Analysis of the effects of HIV-1 Tat on the survival and differentiation of vessel wall-derived mesenchymal stem cells. J. Cell. Biochem. 113 (4), 1132–1141.
Gimble, J.M., Zvonic, S., Floyd, Z.E., Kassem, M., Nuttall, M.E., 2006. Playing with bone and fat. J. Cell. Biochem. 98 (2), 251–266.
Guedia, J., Brun, P., Bhave, S., Fitting, S., Kang, M., Dewey, W.L., Hauser, K.F., Akbarali, H.I., 2016. HIV-1 Tat exacerbates lipopolysaccharide-induced cytokine release via TLR4 signaling in the enteric nervous system. Sci. Rep. 6, 31203.
Hermouet, S., Corre, I., Lippert, E., 2000. Interleukin-8 and other agonists of Gi2 proteins: autocrine paracrine growth factors for human hematopoietic progenitors acting in synergy with colony stimulating factors. Leuk. Lymphoma 38 (1-2), 39–48.
Hofmeister, C.C., Zhang, J., Knight, K.L., Le, P., Stiff, P.J., 2007. Ex vivo expansion of umbilical cord blood stem cells for transplantation: growing knowledge from the hematopoietic niche. Bone Marrow Transplant. 39 (1), 11–23.
Huang, K., Zhou, D.H., Huang, S.L., Liang, S.H., 2005. Age-related biological characteristics of human bone marrow mesenchymal stem cells from different age donors. Zhongguo Shi Yan Xue Ye Xue Za Zhi 13 (6), 1049–1053.
Isern, J., Martín-Antonio, B., Ghazanfari, R., Martín, A.M., López, J.A., del Toro, R., Sánchez-Aguilera, A., Arranz, L., Martín-Pérez, D., Suárez-Lledó, M., Marín, P., Van Pel, M., Fibbe, W.E., Vázquez, J., Scheding, S., Urbano-Ispizúa, Á., Méndez-Ferrer, S., 2013. Self-renewing human bone marrow mesenspheres promote hematopoietic stem cell expansion. Cell Rep. 3 (5), 1714–1724.
Ivanovic, Z., Boiron, J.M., 2009. Ex vivo expansion of hematopoietic stem cells: concept and clinical benefit. Transfus. Clin. Biol. 16 (5–6), 489–500.
Johnson, T.P., Patel, K., Johnson, K.R., Maric, D., Calabresi, P.A., Hasbun, R., Nath, A., 2013. Induction of IL-17 and nonclassical T-cell activation by HIV-Tat protein. Proc. Nat. Acad. Sci. U.S.A 110 (33), 13588–13593.
Ju, S.M., Goh, A.R., Kwon, D.J., Youn, G.S., Kwon, H.J., Bae, Y.S., Choi, S.Y., Park, J., 2012. Extracellular HIV-1 Tat induces human beta-defensin-2 production via NFkappaB/ AP-1 dependent pathways in human B cells. Mol. Cells 33 (4), 335–341.
Kuller, L.H., Tracy, R., Belloso, W., De Wit, S., Drummond, F., Lane, H.C., Ledergerber, B., Lundgren, J., Neuhaus, J., Nixon, D., Paton, N.I., Neaton, J.D., INSIGHT SMART Study Group, 2008. Inflammatory and coagulation biomarkers and mortality in patients with HIV infection. PLoS Med. 5 (10), e203.
Larrick, J.W., Mendelsohn, A.R., 2017. Mesenchymal stem cells for frailty? Rejuvenation Res. 20 (6), 525–529.
Masuda, S., Izpisua Belmonte, J.C., 2013. Cotransplantation of MSCs and HSCs. Transplantation 95 (10), e62–3.
Morini, M., Benelli, R., Giunciuglio, D., Carlone, S., Arena, G., Noonan, D.M., Albini, A., 2000. Kaposi's sarcoma cells of different etiologic origins respond to HIV-Tat through the Flk-1/KDR (VEGFR-2): relevance in AIDS-KS pathology. Biochem. Biophys. Res. Commun. 273 (1), 267–271.
Morrison, S.J., Scadden, D.T., 2014. The bone marrow niche for haematopoietic stem cells. Nature 505 (7483), 327–334.
Nazari-Shafti, T.Z., Freisinger, E., Roy, U., Bulot, C.T., Senst, C., Dupin, C.L., Chaffin, A.E., Srivastava, S.K., Mondal, D., Alt, E.U., Izadpanah, R., 2011. Mesenchymal stem cell derived hematopoietic cells are permissive to HIV-1 infection. Retrovirology 8 (1), 3.
Opi, S., Péloponèse, J.M.Jr., Esquieu, D., Campbell, G., de Mareuil, J., Walburger, A., Solomiac, M., Grégoire, C., Bouveret, E., Yirrell, D.L., Loret, E.P., 2002. Tat HIV-1 primary and tertiary structures critical to immune response against non- homologous variants. J. Biol. Chem. 277 (39), 35915–35919.
Opie, J., 2012. Haematological complications of HIV infection. S. Afr. Med. J. 102 (6), 465–468.
Park, I.W., Wang, J.F., Groopman, J.E., 2001. HIV-1 Tat promotes monocyte chemoattractant protein-1 secretion followed by transmigration of monocytes. Blood 97 (2), 352–358.
Poncin, G., Beaulieu, A., Humblet, C., Thiry, A., Oda, K., Boniver, J., Defresne, M.P., 2012. Characterization of spontaneous bone marrow recovery after sublethal total body irradiation: importance of the osteoblastic/adipocytic balance. PLoS One 7 (2), e30818.
Redig, A.J., Berliner, N., 2013. Pathogenesis and clinical implications of HIV- related anemia in 2013. Hematol. Am. Soc. Hematol. Educ. Program 2013, 377–381.
Scott, S.B., 2010. Emergency department management of hematologic and oncologic complications in the patient infected with HIV. Emerg. Med. Clin. North Am. 28 (2), 325–333.
Shi, X., Hamrick, M., Isales, C.M., 2007. Energy balance, myostatin, and GILZ: factors regulating adipocyte differentiation in belly and bone. PPAR Res. 2007, 92501.
Sloand, E., 2005. Hematologic complications of HIV infection. AIDS Rev. 7 (4), 187–196.
Tsuboi, I., Morimoto, K., Hirabayashi, Y., Li, G.X., Aizawa, S., Mori, K.J., Kanno, J., Inoue, T., 2004. Senescent B lymphopoiesis is balanced in suppressive homeostasis: decrease in interleukin-7 and transforming growth factor-beta levels in stromal cells of senescence-accelerated mice. Exp. Biol. Med. (Maywood) 229 (6), 494–502.
Vasko, T., Frobel, J., Lubberich, R., Goecke, T.W., Wagner, W., 2016. iPSC-derived mesenchymal stromal cells are less supportive than primary MSCs for co-culture of hematopoietic progenitor cells. J. Hematol. Oncol. 9, 43.
Wang, X.L., Hu, P., Guo, X.R., Yan, D., Yuan, Y., Yan, S.R., Li, D.S., 2014. Reprogramming human umbilical cord mesenchymal stromal cells to islet-like cells with the use of in vitroesynthesized pancreatic-duodenal homebox 1 messenger RNA. Cytotherapy 16 (11), 1519–1527.
Weimar, I.S., Miranda, N., Muller, E.J., Hekman, A., Kerst, J.M., de Gast, G.C., Gerritsen, W.R., 1998. Hepatocyte growth factor/scatter factor (HGF/SF) is produced by human bone marrow stromal cells and promotes proliferation, adhesion and survival of human hematopoietic progenitor cells (CD34+). Exp. Hematol. 26 (9), 885–894.
Wilhelm, E., Doyle, M.C., Nzaramba, I., Magdzinski, A., Dumais, N., Bell, B., 2012. CTGC motifs within the HIV core promoter specify Tat-responsive pre-initiation complexes. Retrovirology 9, 62.
Wu, K.H., Sheu, J.N., Wu, H.P., Tsai, C., Sieber, M., Peng, C.T., Chao, Y.H., 2013. Cotransplantation of umbilical cord-derived mesenchymal stem cells promote hematopoietic engraftment in cord blood transplantation: a pilot study. Transplantation 95 (5), 773–777.
Yuan, Y.H., Zhao, S.S., Wang, X.L., Teng, Z.P., Li, D.S., Zeng, Y., 2017. HIV-1 p55-gag protein induces senescence of human bone marrow mesenchymal stem cells and reduces their capacity to support expansion of hematopoietic stem cells in vitro. Cell Biol. Int. 41 (9), 969–981.
Zhu, R.J., Wu, M.Q., Li, Z.J., Zhang, Y., Liu, K.Y., 2013. Hematopoietic recovery following chemotherapy is improved by BADGE-induced inhibition of adipogenesis. Int. J. Hematol. 97 (1), 58–72.